Stable collective charging of ultracold-atom quantum batteries

Abel Rojo-Francàs [1,2,*] Felipe Isaule [3,†] Alan C. Santos [4,‡] Bruno Juliá-Díaz [1,2,§] and Nikolaj Thomas Zinner [5,‖]

[1]*Departament de Física Quàntica i Astrofísica, Facultat de Física, Universitat de Barcelona, 08028 Barcelona, Spain*

[2]*Institut de Ciències del Cosmos, Universitat de Barcelona, Martí i Franquès 1, 08028 Barcelona, Spain*

[3]*Instituto de Física, Pontificia Universidad Católica de Chile, Avenida Vicuña Mackenna 4860, Santiago, Chile*

[4]*Instituto de Física Fundamental, Consejo Superior de Investigaciones Científicas, Calle Serrano 113b, 28006 Madrid, Spain*

[5]*Department of Physics and Astronomy, Aarhus University, 8000 Aarhus C, Denmark*

(Received 18 June 2024; accepted 22 August 2024; published 6 September 2024)

We propose a quantum battery realized with a few interacting particles in a three-well system with different on-site energies, which could be realized with ultracold-atom platforms. We prepare the initial state in the lowest-energy well and charge the battery using a spatial-adiabatic-passage–based protocol, enabling the population of a higher-energy well. We examine the charging under varying interaction strengths and reveal that the consideration of collective charging results in an intriguing oscillatory behavior of the final charge for finite interactions, through diabatic evolution. Our findings provide an opportunity for building stable and controllable quantum batteries.

DOI: 10.1103/PhysRevA.110.032205

I. INTRODUCTION

Energy storing quantum devices [1,2] emerged as part of a quantum energy initiative for quantum-inspired technologies [3], where the energy stored in these quantum batteries (QBs) would be used for further transfer to quantum consumption hubs. The performance of QBs is mainly ruled by laws of quantum thermodynamics, which dictates physical processes involving entropy production, heat, and work in the quantum realm [4]. Through this theory, one may properly manage useful work provided by quantum systems at the single-atom level [5] and the energy cost to perform quantum tasks [6,7] and to predict the extractable amount of work stored in such systems [8], among other applications [9]. By harnessing genuine effects from interacting quantum systems, QBs exhibit scalable enhanced charging performance (power) with respect to their noninteracting (classical) counterpart [10–22]. Experimental realizations of QBs have been done with superconducting integrated circuits [23,24], nuclear magnetic resonance [25], quantum dots [26], and organic microcavities [27], with the first experiment of a room-temperature QB designed with carboxylate-based metal complexes [28].

Despite the high performance of these devices, some properties of such devices make their usage for real-world applications a challenge. In particular, instantaneous discharging, the main focus of this work, is observed for always-on charging of QBs due to the quantum recurrence theorem of Poincaré [29], demanding then for the development of stable charging strategies. The instantaneous discharging is related to oscillations in time of the stored energy in the battery, leading to loss of performance due to the energy backflow from the battery to the charger [30]. Proposals of stable charging of QBs have been induced through localization effects in disordered spin systems [31,32], using single [33] and collective dark states [34], Zeno protection [35], adiabatic evolutions [33,36], the nonreciprocal approach [37], and transitionless driving [30], for example, with the first experimental implementation of optimal stable charging done with superconducting three-level atoms [23]. Inspired by QB proposals with interacting spin chains [38–41], ultracold atoms confined in optical lattices appear as a promising platform for designing QBs [42]. The high level of control offered by ultracold atoms [43–46] makes them unique candidates for developing efficient and stable QBs. In particular, the control over the atomic internal states and of the interatomic interactions offer novel configurations of QBs not achievable with other quantum physical systems.

In this article we propose a three-well QB controlled with a protocol based on spatial adiabatic passage (SAP) [47–49], as depicted in Fig. 1(a). The SAP implementation is already possible in ultracold-atom laboratories [50]. Moreover, and in contrast to previous related studies [33], we consider quantum collective effects by including on-site interactions. The interaction effects cause the time evolution to no longer be adiabatic. However, since we are using the SAP order of applying the couplings and the final target state, we refer to our setup as an SAP-based protocol. Our protocol creates a stable system if we achieve the maximum charge, and in this study we focus on the charging mechanism. In addition to the proposed three-well implementation, such a QB could also be realized with an array of three-level systems with a protocol based on stimulated Raman adiabatic passage [51,52].

*Contact author: abel.rojo@fqa.ub.edu
†Contact author: felipe.isaule@uc.cl
‡Contact author: ac_santos@iff.csic.es
§Contact author: bruno@fqa.ub.edu
‖Contact author: zinner@phys.au.dk

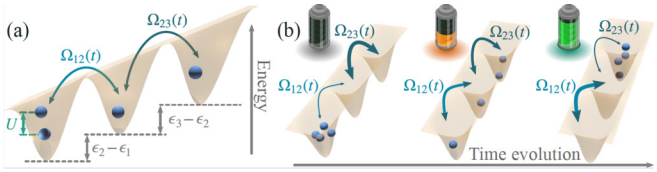

FIG. 1. (a) Physical system consisting of N particles which may populate three wells with different energy. (b) Schematic representation of the evolution used for the stable charging protocol, in which the tunneling strengths $\Omega_{12}(t)$ and $\Omega_{23}(t)$ are switched on in a counterintuitive way to avoid populating the intermediate well with energy ϵ_2.

This article is organized as follows. In Sec. II we present the model we are working with, including the Hamiltonian and the charge definition. In Sec. III we explore how the interaction affects the charging protocol. In Sec. IV we use analytical models to explain the effects of the interaction on the charge, being exact for the two-particle case and an approximation for a larger number of particles. In Sec. V we summarize our work and present the conclusions.

II. MODEL

We consider as a general case N identical bosons in a three-well system, where the wells energy is ϵ_i, with $i = 1$–3 in ascending order. In addition, we consider an energy U when a pair of particles is in the same well. On top of that, our SAP-inspired protocol considers a time-dependent tunneling between wells 1 and 2 and also between wells 2 and 3. As illustrated in Fig. 1, the Hamiltonian in a second quantization formalism reads $\hat{H} = \hat{H}_0 + \hat{H}_{\rm coll} + \hat{H}_{\rm ch}$, where $\hat{H}_0 = \sum_{i=1}^{3} \epsilon_i \hat{b}_i^\dagger \hat{b}_i$ is the self-Hamiltonian of the system that sets the energy scale of the battery, $\hat{H}_{\rm coll} = \frac{1}{2} U \sum_{i=1}^{3} \hat{n}_i(\hat{n}_i - 1)$ is the *in situ* particle-particle interaction that describes the collective (quantum) aspect of the battery charging, and the charging $\hat{H}_{\rm ch}$ describes the time-dependent tunneling between wells

$$\hat{H}_{\rm ch} = \Omega_{12}(t) e^{i\omega_{12}t} \hat{b}_1^\dagger \hat{b}_2 + \Omega_{23}(t) e^{i\omega_{23}t} \hat{b}_2^\dagger \hat{b}_3 + \text{H.c.}, \qquad (1)$$

where $\hat{b}_i^\dagger$ ($\hat{b}_i$) is the creation (annihilation) operator of a particle in the well i and $\hat{n}_i = \hat{b}_i^\dagger \hat{b}_i$ is the number operator. The coupling is assumed to have driving strength $\Omega_{ij}(t)$ in resonance with the energy transitions of the system at a frequency $\omega_{ij} = (\epsilon_j - \epsilon_i)/\hbar$. The SAP is implemented by the suitable choice of the tunneling such that $\Omega_{12}(0) = \Omega_{23}(\tau) = 0$ and $\Omega_{12}(\tau), \Omega_{23}(0) \neq 0$. Here we choose a lineal transition given by $\Omega_{12}(t) = t\Omega/\tau$ and $\Omega_{23}(t) = \Omega - \Omega_{12}(t)$. So, according to the adiabatic theorem [53], for large enough τ the system will move the particles from the lowest- to the highest-energy well.

At the end of the charging, the extractable amount of energy by coherent drives from a QB is defined by ergotropy [8], which for a unitary evolution charging can be uniquely obtained as [36]

$$C = \langle \Psi(\tau) | \hat{H}_0 | \Psi(\tau) \rangle, \qquad (2)$$

where $|\Psi(\tau)\rangle$ is the state at the end of the SAP protocol. By exploiting the definition of battery capacity as the energy of the most active state [54], it is possible to get the maximum charge for our system with N particles as $C_{\rm max.} = N\epsilon_3$, corresponding to an eigenstate of the final Hamiltonian and thus stable. The energy charging of the QB may be obtained from the Schrödinger equation in the interaction picture as

$$\hat{H}_{\rm int} = \hat{H}_{\rm coll} + \hbar\Omega_{12}(t)\hat{b}_1^\dagger \hat{b}_2 + \hbar\Omega_{23}(t)\hat{b}_2^\dagger \hat{b}_3 + \text{H.c.}, \qquad (3)$$

and thus the charging performance depends only on the tunneling amplitudes and the collectivity parameter U.

III. INTERACTING SYSTEM CHARGE

Now we analyze the final charge diagram as a function of the coupling $\tau\Omega$ and the internal interaction τU. In Fig. 2 we show the charge diagram corresponding to $N = 2$–4. The charge only depends on the absolute value of the interaction $|U|$, but not on its sign. The energy spectra are computed with negative interactions $U < 0$ for description simplicity, but the physics is the same for $U > 0$.

First, we note that the noninteracting limit $U = 0$ (left side of the panels) corresponds to the single-particle configuration studied with a stimulated Raman adiabatic passage protocol in Ref. [33], which does not consider collective charging. For $|U| > 0$, Fig. 2 shows two distinct regions. On one side, when the coupling $\tau\Omega$ is much smaller than the interaction τU (bottom right regions of the panels), the system ends with essentially a null final charge ($C \approx 0$). On the other hand, when the coupling is much larger than the interaction (top regions of the panels), the system produces a finite final charge C but also shows an intriguing oscillation of C with increasing $\tau|U|$ between maximum and partial charging.

To understand why the system does not charge in the weak tunneling region, we examine the system with $N = 2$, even though our arguments can be generalized for more particles. A system with two bosons on a triple-well potential has six states in its Hilbert space. Due to the large interaction U, the system will form two manifolds, one with the three states with the particles in the same well and the other with both particles in different wells. Both manifolds are separated by an energy gap approximately equal to U. In addition, our tunneling is a single-particle operator and thus it can only move the particles individually. The latter connects the states with two particles in the same well to states with particles at different wells. If the coupling is weak compared with the gap between the states that are connecting, the transition is almost suppressed. Therefore, by starting from both particles in the lowest-energy well, if $U \gg \Omega$ the state cannot evolve with time, and thus both particles remain in the same initial site during the evolution, preventing charging.

In the second region, where the coupling is much larger than the interaction (above the red solid line in the panels), the results do not depend on the value of the coupling $\tau\Omega$. We find oscillations in the charge as a function of $|U|$ for any number of particles N, where the period of these oscillations depends on N. Interestingly, we also find that systems with odd and even numbers of particles show a distinct onset of oscillations with U. Indeed, with even N the oscillations are approximately periodic and with a fixed amplitude. In contrast, for odd N the amplitude of the oscillations decreases but achieves periodic full charging. We will explain this phenomenon later on.

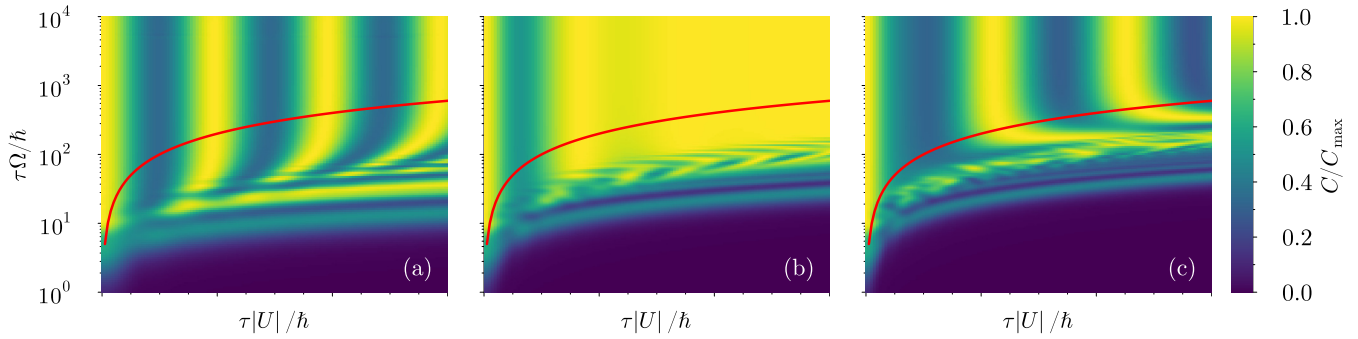

FIG. 2. Normalized final ($t = \tau$) charge $C/C_{\max}$ as a function of the interaction $\tau|U|/\hbar$ and the coupling $\tau\Omega/\hbar$, for (a) $N = 2$, (b) $N = 3$, and (c) $N = 4$. The red solid line on the charge map indicates the line with $|U| = 0.1\Omega$.

Importantly, our results show that it is possible to reach $C_{\max}$ for any N and if one chooses $|U|$ to the regions of maximum charge. This feature could be exploited in experiments to get a full charge by tuning the interatomic interactions. The maximum charge is also achievable for a finite interaction when the interaction strength and the coupling have similar values. That situation is interesting, but we focus on the situation where $\Omega \gg |U|$.

IV. ANALYTICAL TIME EVOLUTION

Having examined the charging from our numerical calculations, we now provide an analytical interpretation of our results. We focus on the case with $\Omega/|U| \gg 1$, corresponding to the region above the red solid lines in Figs. 2(a)–2(c).

We first analyze the two-particle case, which can be examined analytically for $\Omega/|U| \gg 1$. By taking t as a fixed parameter in Eq. (3), we can diagonalize the Hamiltonian for two particles analytically, resulting in an energy spectrum like the one shown in Fig. 3. The spectrum has states with an energy proportional to $\pm\Omega$ and others to $\pm 2\Omega$. While these states show a weak dependence on U and t/τ, the gap between these states is approximately Ω. In addition, at the center of Fig. 3(a) the spectrum shows two states whose energy does not depend on the coupling Ω but depends instead on U. These two states can be better appreciated in Fig. 3(b). Moreover, at $t = 0$, the state with both particles in the lowest-energy well (our initial state $|\varphi_0\rangle$) is an eigenstate with energy $E = U$, belonging to the central manifold. At $t = \tau$, the state with both particles in the higher-energy well (the state with maximum charge $|\varphi_1\rangle$) is also an eigenstate with energy $E = U$, belonging to the central manifold as well.

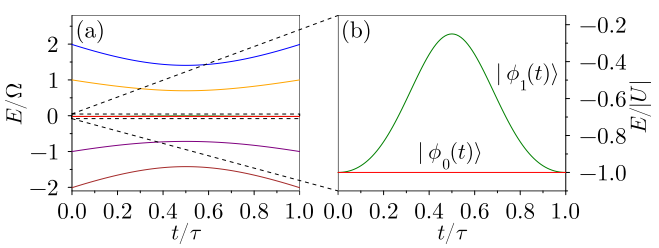

FIG. 3. Energy spectrum for two particles with interaction $U = -0.02\Omega$: (a) the complete energy spectrum for E/Ω and (b) close-up of the two states in the central manifold for E/U.

Therefore, the battery starts from a state in the central manifold, disconnected from the other states by a factor Ω. If the coupling Ω is much larger than the energy scales of the central manifold (U), one can expect that all the physics will happen through the two states of Fig. 3(b). From now on, we will refer to them as $|\phi_0(t)\rangle$ with energy $E_0(t)$ and $|\phi_1(t)\rangle$ with energy $E_1(t)$. These states are the instantaneous eigenstates of the Hamiltonian. The state $|\phi_0\rangle$ does not depend on time and has a constant energy $E_0(t) = U$, while $|\phi_1\rangle$ is time dependent.

By computing the time evolution of the state in a superposition between $|\phi_0\rangle$ and $|\phi_1\rangle$ with the parallel transport condition [55], the final ergotropy is

$$C = C_{\max}\{1 - \beta \sin^2[3(\pi - 4)\tau U/16\hbar]\}, \tag{4}$$

with $\beta = 4(2\epsilon_3 - \epsilon_1 - \epsilon_2)/9\epsilon_3$ (see Appendix A). As in Fig. 2(a), Eq. (4) shows oscillations as a function of τU. In Fig. 4 we show a comparison between the results obtained with the numeric time evolution and the results from the analytic result (4). We observe almost perfect agreement for large $\Omega\tau$, while we observe increasing discrepancies for decreasing $\Omega\tau$, as expected.

Now we turn our attention to the general $N > 2$ case, which can be analyzed with an effective theory. Once we add more particles, the spectral properties observed with $N = 2$ become slightly different. However, the main argument is similar; the system has a set of states with an energy proportional to Ω, whereas a few of them do not depend on that coupling.

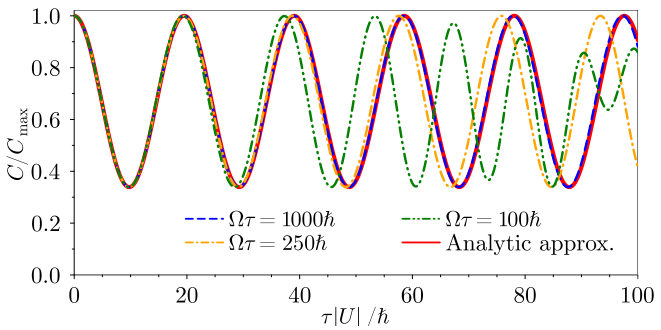

FIG. 4. Charge as a function of the interaction $\tau|U|/\hbar$ for $N = 2$. The red solid line shows the analytical result (4) for large $\Omega\tau$, while the other lines show numerical calculations for the indicated values of $\tau\Omega$.

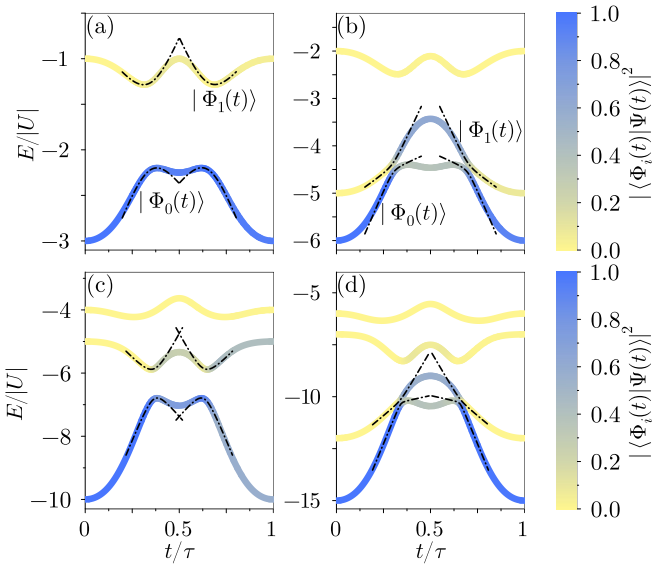

FIG. 5. Energy spectrum for (a) $N = 3$, (b) $N = 4$, (c) $N = 5$, and (d) $N = 6$ and its population (in color) corresponding to a time evolution with parameters $\tau U = -20\hbar$ and $\tau\Omega = 1000\hbar$. The dash-dotted lines are the fit corresponding to the energies of Eq. (7). Only the equivalent states of Fig. 3(b) are shown.

For $N = 2$ only two states do not depend on Ω [Fig. 3(b)]. However, we find that for N particles $\lfloor N/2 + 1 \rfloor$ states fulfill such condition.

In Fig. 5 we show these states for several numbers of particles, from $N = 3$ to $N = 6$. In contrast to Fig. 3(b), here the states are not degenerate at the beginning and the end of the protocol. In that case, our initial state at $t = 0$ and our target state at $t = \tau$ correspond to states with energy $E/U = N(N-1)/2$ and thus in Fig. 5 can be identified as the manifold ground state.

In Fig. 5 the colors show the probability associated with each instantaneous eigenstate $|\Phi_i(t)\rangle$ for a time evolution. We obtain a slight difference between the odd and even numbers of particles, as we observed in the charge diagrams from Fig. 2. For an odd N, the minimum gap between the manifold ground state (the initial state) and the first excitation of that manifold one is on the order of U. On the other hand, for systems with even N, the minimum gap is approximately $0.2U$. The latter indicates that for an odd N it is easier to have an adiabatic evolution due to the larger gap. For the limit of large N, even if the gaps still remain with the same ratios, the relative gaps will vanish. As the total energy scales as N^2, the differences between odd and even numbers of particles will disappear in the thermodynamic limit.

For these systems, we have modeled an effective two-level model of the time evolution. In that situation, the initial state (from now on $|\Phi_0\rangle$) in Fig. 5 has an avoided crossing with the first excitation of the manifold (from now on $|\Phi_1\rangle$) at $t \sim 0.3\tau \equiv \tau_0$ and also at $t \sim 0.7\tau \equiv \tau_1$. In the general case, we define τ_0 and τ_1 as the times where the gap is minimum. One can assume that the evolution is adiabatic and there is a level transition only at the avoided crossings, with the same probabilities at both times. We also assume that all the relevant physics occurs between these two states, ignoring the rest.

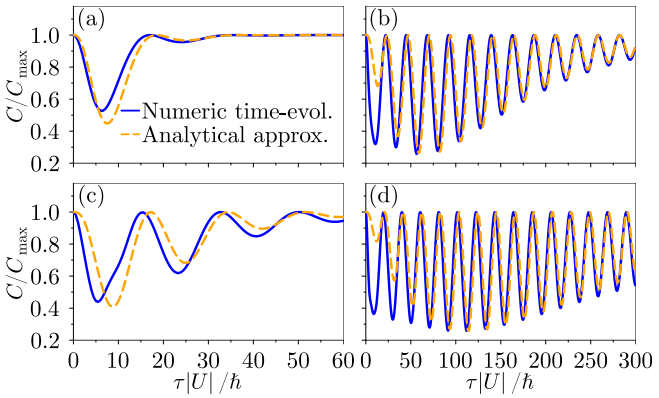

FIG. 6. Charge as a function of the interaction U for (a) $N = 3$, (b) $N = 4$, (c) $N = 5$, and (d) $N = 6$ computed with $\tau\Omega = 10000\hbar$. Blue solid lines correspond to the numerical time-evolution calculations and the orange dashed lines to the predictions of the model of Eq. (5), where the probability is computed using Eq. (6).

With that mechanism, by assuming that transitions may occur in an avoided crossing with probability $P_\updownarrow$, it is possible to show that the final ergotropy is (see Appendix B)

$$\frac{C}{C_{\max}} = 1 - 4c\bar{P}_\updownarrow P_\updownarrow \sin^2\left(\int_{\tau_0}^{\tau_1}(E_0 - E_1)dt/2\hbar\right), \quad (5)$$

where $c = 1 - \langle\Phi_1|H_0|\Phi_1\rangle/\langle\Phi_0|H_0|\Phi_0\rangle$ and $\bar{P}_\updownarrow = 1 - P_\updownarrow$, with $P_\updownarrow$ given by the Landau-Zener transition probability

$$P_\updownarrow = \exp(-2\pi a^2/\hbar|\alpha|), \quad (6)$$

where both a and α are obtained by the adjustment in the lowest gap in the spectrum of the two states considered. Near the transition, in the Landau-Zener approximation, the energy of the states is

$$E(t) = \tfrac{1}{2}[(k_1 + k_2)t \pm \sqrt{4a^2 + (k_1 - k_2)^2 t^2}], \quad (7)$$

where we fit the parameters α, k_1, and k_2 and we compute $\alpha = k_1 - k_2$. We plot the lines of the energy obtained in the fit as dash-dotted lines in Fig. 5.

In Fig. 6 we compare the numerical results of the final charge as a function of τU for a large value of $\tau\Omega$ with the predictions of the two-level model using the Landau-Zener transition probability. With our model, we only use information about the energy spectrum. We obtain good agreement with the numerical time-evolution simulation, especially on the frequency of the oscillations, but also in the decay of the amplitude with more accurate results for $N = 3$ and 4. We observe a discrepancy for small interactions and also in the decay of the amplitude for large interactions, indicating that the two-level model is more robust for intermediate U.

V. CONCLUSION

In this article we have shown how a battery based on a three-well system charges when we consider the interaction. We have demonstrated that it is possible to reach the maximum charge for a finite value of the interaction through a diabatic procedure. In addition, we have explained the time

evolution of the system with simple models that use only the information of the energy spectrum. Our quantum battery proposal is feasible experimentally in ultracold-atom laboratories nowadays.

A future perspective to extend this study could be to explore the effects of temperature and check if the battery remains stable. Additionally, it could be interesting to examine the effects of a larger chain, opening the possibility to study the effect of fermionic statistics.

ACKNOWLEDGMENTS

We acknowledge helpful discussions with Joan Martorell and Verònica Ahufinger. B.J-D and A.R-F acknowledge funding from MCIN/AEI/10.13039/5011 00011033, through Grant No. PID2020-114626GB-I00, and the Unit of Excellence María de Maeztu 2020–2023 award to the Institute of Cosmos Sciences, through Grant No. CEX2019-000918-M, funded by MCIN/AEI/10.13039/501100011033. We acknowledge financial support from the Generalitat de Catalunya (Grant No. 2021SGR01095). A.R-F acknowledges funding from MIU through Grant No. FPU20/06174. F.I. acknowledges funding from ANID through FONDECYT Postdoctorado Grant No. 3230023. A.C.S acknowledges support from the European Union's Horizon 2020 FET-Open project SuperQuLAN (Grant No. 899354) and from the Proyecto Sinérgico CAM 2020 (NanoQuCo-CM) Grant No. Y2020/TCS-6545 from the Comunidad de Madrid. N.T.Z. acknowledges support from the Independent Research Fund Denmark and the Novo Nordisk Foundation.

APPENDIX A: DEVELOPMENT OF THE TWO-PARTICLE TIME EVOLUTION

Our initial state $|\varphi\rangle$ can be expressed as a superposition of both states $|\phi_0(t=0)\rangle$ and $|\phi_1(t=0)\rangle$ as

$$|\Phi(t=0)\rangle = |\varphi\rangle = \sqrt{\tfrac{1}{3}}|\phi_0(t=0)\rangle + \sqrt{\tfrac{2}{3}}|\phi_1(t=0)\rangle. \tag{A1}$$

Assuming an adiabatic evolution with the parallel transport condition $\langle\phi_i|\frac{\partial}{\partial t}\phi_i\rangle = 0$, the time evolution of the state can be expressed as

$$|\Phi(t)\rangle = \sqrt{\tfrac{1}{3}}\exp\left(-i\int E_0(t)dt/\hbar\right)|\phi_0(t)\rangle + \sqrt{\tfrac{2}{3}}\exp\left(-i\int E_1(t)dt/\hbar\right)|\phi_1(t)\rangle, \tag{A2}$$

and taking into account that E_0 is constant, we can rearrange it as

$$|\Phi(t)\rangle = \sqrt{\tfrac{1}{3}}|\phi_0(t)\rangle + \sqrt{\tfrac{2}{3}}\exp\left(-i\int [E_1(t)-E_0]dt/\hbar\right)|\phi_1(t)\rangle. \tag{A3}$$

Now, by computing the integral from $t=0$ to $t=\tau$, we obtain the state at the end of the SAP protocol:

$$|\Phi(\tau)\rangle = \sqrt{\tfrac{1}{3}}|\phi_0(\tau)\rangle + \sqrt{\tfrac{2}{3}}e^{-i3(\pi-4)\tau U/8\hbar}|\phi_1(\tau)\rangle. \tag{A4}$$

Note that the final state is also described by the two instantaneous time eigenstates with a relative phase proportional to τU. Using this state, we can recover the charge using our definition.

APPENDIX B: DEVELOPMENT OF THE FEW-PARTICLE TIME EVOLUTION

Using the two-level model, the time-dependent state will be

$$|\Psi(t<\tau_0)\rangle = |\Psi_0\rangle, \tag{B1}$$

until the first crossing. After that, there will be a transition with probability $P_\updownarrow$ and so the state just after the transition will be

$$|\Psi(t=\tau_0)\rangle = \sqrt{(1-P_\updownarrow)}|\Psi_0\rangle + \sqrt{P_\updownarrow}|\Psi_1\rangle; \tag{B2}$$

with a parallel transport, we assume an adiabatic evolution until the second transition. So the state will arrive with the phases

$$|\Psi(\tau_0<t<\tau_1)\rangle = \sqrt{(1-P_\updownarrow)}\exp\left(-i\int_{\tau_0}^{t} E_0 dt/\hbar\right)|\Psi_0\rangle + \sqrt{P_\updownarrow}\exp\left(-i\int_{\tau_0}^{t} E_1 dt/\hbar\right)|\Psi_1\rangle. \tag{B3}$$

After the second transition, we can express the state as

$$|\Psi(t\geqslant\tau_1)\rangle = \left[P_\updownarrow + (1-P_\updownarrow)\exp\left(-i\int_{\tau_0}^{\tau_1}(E_0-E_1)dt/\hbar\right)\right]|\Psi_0\rangle + \sqrt{P_\updownarrow(1-P_\updownarrow)}\left[1-\exp\left(-i\int_{\tau_0}^{\tau_1}(E_0-E_1)dt/\hbar\right)\right]|\Psi_1\rangle. \tag{B4}$$

Note the negative sign in the second term. This sign is needed to preserve the norm of the wave function and it comes from the relative phase in the transition. With this state, we can derive the charge at $t=\tau$.

[1] R. Alicki and M. Fannes, Phys. Rev. E **87**, 042123 (2013).
[2] F. C. Binder, S. Vinjanampathy, K. Modi, and J. Goold, New J. Phys. **17**, 075015 (2015).
[3] A. Auffèves, PRX Quantum **3**, 020101 (2022).
[4] S. Deffner and S. Campbell, *Quantum Thermodynamics: An Introduction to the Thermodynamics of Quantum Information* (Morgan & Claypool, Williston, 2019).
[5] J. Roßnagel, S. T. Dawkins, K. N. Tolazzi, O. Abah, E. Lutz, F. Schmidt-Kaler, and K. Singer, Science **352**, 325 (2016).

[6] J. Monsel, M. Fellous-Asiani, B. Huard, and A. Auffèves, Phys. Rev. Lett. **124**, 130601 (2020).
[7] S. Deffner, Europhys. Lett. **134**, 40002 (2021).
[8] A. E. Allahverdyan, R. Balian, and T. M. Nieuwenhuizen, Europhys. Lett. **67**, 565 (2004).
[9] N. M. Myers, O. Abah, and S. Deffner, AVS Quantum Sci. **4**, 027101 (2022).
[10] F. Barra, Phys. Rev. Lett. **122**, 210601 (2019).
[11] G. M. Andolina, M. Keck, A. Mari, M. Campisi, V. Giovannetti, and M. Polini, Phys. Rev. Lett. **122**, 047702 (2019).
[12] D. Ferraro, M. Campisi, G. M. Andolina, V. Pellegrini, and M. Polini, Phys. Rev. Lett. **120**, 117702 (2018).
[13] F. Campaioli, F. A. Pollock, F. C. Binder, L. Céleri, J. Goold, S. Vinjanampathy, and K. Modi, Phys. Rev. Lett. **118**, 150601 (2017).
[14] A. Crescente, M. Carrega, M. Sassetti, and D. Ferraro, Phys. Rev. B **102**, 245407 (2020).
[15] M. Carrega, A. Crescente, D. Ferraro, and M. Sassetti, New J. Phys. **22**, 083085 (2020).
[16] J.-Y. Gyhm and U. R. Fischer, AVS Quantum Sci. **6**, 012001 (2024).
[17] J.-Y. Gyhm, D. Šafránek, and D. Rosa, Phys. Rev. Lett. **128**, 140501 (2022).
[18] J. Kim, J. Murugan, J. Olle, and D. Rosa, Phys. Rev. A **105**, L010201 (2022).
[19] D. Rossini, G. M. Andolina, D. Rosa, M. Carrega, and M. Polini, Phys. Rev. Lett. **125**, 236402 (2020).
[20] D. Rosa, D. Rossini, G. M. Andolina, M. Polini, and M. Carrega, J. High Energy Phys. 11 (2020) 067.
[21] V. Shaghaghi, V. Singh, G. Benenti, and D. Rosa, Quantum Sci. Technol. **7**, 04LT01 (2022).
[22] C. Rodríguez, D. Rosa, and J. Olle, Phys. Rev. A **108**, 042618 (2023).
[23] C.-K. Hu, J. Qiu, P. J. P. Souza, J. Yuan, Y. Zhou, L. Zhang, J. Chu, X. Pan, L. Hu, J. Li, Y. Xu, Y. Zhong, S. Liu, F. Yan, D. Tan, R. Bachelard, C. J. Villas-Boas, A. C. Santos, and D. Yu, Quantum Sci. Technol. **7**, 045018 (2022).
[24] G. Gemme, M. Grossi, D. Ferraro, S. Vallecorsa, and M. Sassetti, Batteries **8**, 43 (2022).
[25] J. Joshi and T. S. Mahesh, Phys. Rev. A **106**, 042601 (2022).
[26] I. Maillette de Buy Wenniger, S. E. Thomas, M. Maffei, S. C. Wein, M. Pont, N. Belabas, S. Prasad, A. Harouri, A. Lemaître, I. Sagnes, N. Somaschi, A. Auffèves, and P. Senellart, Phys. Rev. Lett. **131**, 260401 (2023).
[27] J. Q. Quach, K. E. McGhee, L. Ganzer, D. M. Rouse, B. W. Lovett, E. M. Gauger, J. Keeling, G. Cerullo, D. G. Lidzey, and T. Virgili, Sci. Adv. **8**, eabk3160 (2022).
[28] C. Cruz, M. F. Anka, M. S. Reis, R. Bachelard, and A. C. Santos, Quantum Sci. Technol. **7**, 025020 (2022).
[29] P. Bocchieri and A. Loinger, Phys. Rev. **107**, 337 (1957).
[30] L. F. C. Moraes, A. Saguia, A. C. Santos, and M. S. Sarandy, Europhys. Lett. **136**, 23001 (2021).
[31] M. B. Arjmandi, H. Mohammadi, A. Saguia, M. S. Sarandy, and A. C. Santos, Phys. Rev. E **108**, 064106 (2023).
[32] D. Rossini, G. M. Andolina, and M. Polini, Phys. Rev. B **100**, 115142 (2019).
[33] A. C. Santos, B. Çakmak, S. Campbell, and N. T. Zinner, Phys. Rev. E **100**, 032107 (2019).
[34] J. Q. Quach and W. J. Munro, Phys. Rev. Appl. **14**, 024092 (2020).
[35] S. Gherardini, F. Campaioli, F. Caruso, and F. C. Binder, Phys. Rev. Res. **2**, 013095 (2020).
[36] A. C. Santos, A. Saguia, and M. S. Sarandy, Phys. Rev. E **101**, 062114 (2020).
[37] B. Ahmadi, P. Mazurek, P. Horodecki, and S. Barzanjeh, Phys. Rev. Lett. **132**, 210402 (2024).
[38] T. P. Le, J. Levinsen, K. Modi, M. M. Parish, and F. A. Pollock, Phys. Rev. A **97**, 022106 (2018).
[39] S. Ghosh, T. Chanda, and A. Sen(De), Phys. Rev. A **101**, 032115 (2020).
[40] F. Zhao, F.-Q. Dou, and Q. Zhao, Phys. Rev. A **103**, 033715 (2021).
[41] S. Ghosh and A. Sen(De), Phys. Rev. A **105**, 022628 (2022).
[42] T. K. Konar, L. G. C. Lakkaraju, S. Ghosh, and A. Sen(De), Phys. Rev. A **106**, 022618 (2022).
[43] I. Bloch, J. Dalibard, and S. Nascimbène, Nat. Phys. **8**, 267 (2012).
[44] C. Gross and I. Bloch, Science **357**, 995 (2017).
[45] M. Lewenstein, A. Sanpera, and V. Ahufinger, *Ultracold Atoms in Optical Lattices: Simulating Quantum Many-Body Systems* (Oxford University Press, Oxford, 2012).
[46] M. Lewenstein, A. Sanpera, V. Ahufinger, B. Damski, A. Sen(De), and A. Sen, Adv. Phys. **56**, 243 (2007).
[47] C. J. Bradly, M. Rab, A. D. Greentree, and A. M. Martin, Phys. Rev. A **85**, 053609 (2012).
[48] R. Menchon-Enrich, A. Benseny, V. Ahufinger, A. D. Greentree, T. Busch, and J. Mompart, Rep. Prog. Phys. **79**, 074401 (2016).
[49] J. L. Rubio, V. Ahufinger, T. Busch, and J. Mompart, Phys. Rev. A **94**, 053606 (2016).
[50] S. Taie, T. Ichinose, H. Ozawa, and Y. Takahashi, Nat. Commun. **11**, 257 (2020).
[51] N. V. Vitanov, A. A. Rangelov, B. W. Shore, and K. Bergmann, Rev. Mod. Phys. **89**, 015006 (2017).
[52] K. Bergmann, H.-C. Nägerl, C. Panda, G. Gabrielse, E. Miloglyadov, M. Quack, G. Seyfang, G. Wichmann, S. Ospelkaus, A. Kuhn, S. Longhi, A. Szameit, P. Pirro, B. Hillebrands, X.-F. Zhu, J. Zhu, M. Drewsen, W. K. Hensinger, S. Weidt, T. Halfmann *et al.*, J. Phys. B **52**, 202001 (2019).
[53] T. Kato, J. Phys. Soc. Jpn. **5**, 435 (1950).
[54] X. Yang, Y.-H. Yang, M. Alimuddin, R. Salvia, S.-M. Fei, L.-M. Zhao, S. Nimmrichter, and M.-X. Luo, Phys. Rev. Lett. **131**, 030402 (2023).
[55] M. V. Berry, J. Phys. A: Math. Theor. **42**, 365303 (2009).